

# Monitoring of coastal dynamics at Subang Regency using Landsat Collection Data and Cloud Computing Based

*Abd Malik A Madinu*<sup>1,7,\*</sup>, *Naufal Amir Jouhary*<sup>1,7</sup>, *Aulia Ulfa*<sup>2,7</sup>, *Intan Nur Rahmadhanti*<sup>3,7</sup>, *Nihawa Hajar Pudjawati*<sup>4,7</sup>, *Rahmat Asy'Ari*<sup>5,7,8</sup>, *Neviaty P Zamani*<sup>6,7</sup>, *Rahmat Pramulya*<sup>7,9</sup>, and *Yudi Setiawan*<sup>7,10</sup>

<sup>1</sup> Department of Geophysics and Meteorology, Faculty of Mathematics and Natural Science, IPB University, Jl. Agatis Dramaga Bogor, Bogor 16680, Indonesia

<sup>2</sup> Department of Biology, Faculty of Mathematics and Natural Science, IPB University, Jl. Agatis Dramaga Bogor, Bogor 16680, Indonesia

<sup>3</sup> Department of Silviculture, Faculty of Forestry and Environment, IPB University, Jl. Agatis Dramaga Bogor, Bogor 16680, Indonesia

<sup>4</sup> Department of Soil Science and Land Resources, Faculty of Agriculture, IPB University, Jl. Agatis Dramaga Bogor, Bogor 16680, Indonesia

<sup>5</sup> Department of Forest Management, Faculty of Forestry and Environment, IPB University, Jl. Agatis Dramaga Bogor, Bogor 16680, Indonesia

<sup>6</sup> Department of Marine Science and Technology, Faculty of Fisheries and Marine Science, IPB University, Jl. Agatis Dramaga Bogor, Bogor 16680, Indonesia

<sup>7</sup> IPB Sustainable Science Research Student Association - IPB SSRS Association, IPB University, Jl. Agatis Dramaga Bogor, Bogor 16680, Indonesia

<sup>8</sup> CNT Tourism Information and Research Center, Community Nature Traveler - CNT Batui, Banggai Regency 94762, Central Sulawesi, Indonesia

<sup>9</sup> Center for Low Carbon Development, University of Teuku Umar, Aceh, Indonesia

<sup>10</sup> Center for Environmental Science, Institute for Research and Community Empowerment IPB, IPB University, Bogor Regency 16680, Indonesia

**Abstract.** This study aims to better understand the coastal dynamics along the 6.89 km of Subang shoreline using Landsat data and GIS methods with cloud computing-based analysis. The data is processed using remote sensing techniques, image classification, and change detection algorithms. Furthermore, this research harnesses cloud computing to efficiently manipulate big data, enabling rapid and measurable analysis of coastline changes. Cloud computing-based platforms facilitate data storage, processing, and dissemination, enhancing accessibility for researchers and stakeholders. This study indicates that the area has experienced significant changes from 1990 to 2023, with the total length of the coastlines that have changed (positive stands for accretion and negative for erosion) being 8.21 km (-16,86 %) for 1990 to 2000, 6.52 km (16.21%) for 2000 to 2010, 8.14 km (6,66%) for 2010 to 2020, and 8.81 km (-19,16%) for 2020 to 2023. The results provide valuable information about erosion, accretion, and coastal morphological changes. The findings can help make informed decisions for sustainable coastal management. The methodology presented in this article

---

\* Corresponding author: [abd.malik@apps.ipb.ac.id](mailto:abd.malik@apps.ipb.ac.id)

demonstrates a solid approach to coastline monitoring that can be replicated in other areas for more efficient and effective coastal management and environmental preservation.

## 1 Introduction

Coastal is an area alongside the border between the wave-breaking area and the offshore quarter [1]. This area is a transition zone between terrestrial and marine ecosystems. Coastal areas have diverse geological, geomorphological, ecological, and human capabilities. Some examples of coastal capabilities include sandy seashores, coastal marshes, lagoons, estuaries, and coral reefs. Meanwhile, the period shoreline is a dynamic boundary between the ocean and land, constantly converting through the years [2]. The coastline has a various and dynamic form, ensuing in its continuous transformation. Changes within the shoreline can take the shape of accretion, which is the addition of land, and erosion, which is the decrease of land. Both can be caused by natural or anthropogenic (human) factors [3]. Coastal areas have various features, including environmental and ecological capabilities, beach protection functions, recreation and tourism capabilities, financial and fishing features, and transportation functions. This coastal use can cause an issue in the occurrence of erosion. Erosion is a phenomenon of shoreline degradation due to bodily activities, including currents, rain, wind, and human activities [4]. Erosion and accretion impact changes in the shoreline. Changes in the coastline occur since coastal regions have a sensitivity to constantly regulate to gain natural stability against the impacts experienced [5].

Land use change is a regular process with improvement initiatives and intervention fees that purpose land in diverse world components to change [6]. Coastal areas play an essential role in human existence, especially coastal residents because it provides natural resources to serve society. Coastal areas are particular areas inside a landscape framework where the areas land and sea meet [7]. The land is a limited resource that cannot be renewed. Meanwhile, the number of people who need land for their activities occasionally increases. The growth of the people is one thing behind the emergence of irrational land use. Improper land use can cause land harm and even casualties [8]. Coastal and marine regions play an essential function as a supply of profits and are projected to be the focal point of Indonesia's future development. The usage and conservation of potential coastal and marine water resources must be executed rationally and sustainably because it has become a new development model today [9]. Aquaculture has begun toward the south coast of Java. Many new farmers with new land regions have started cultivating vannamei shrimp. Some farmers additionally take advantage of untamed ponds and convert traditional ponds into semi-intensive or in-depth ponds. Previous study has proven that extensive shrimp farming mainly contributes the most essential percentage [51]. Developing coastal land use and shrimp cultivation can grow sustainable livelihoods and decrease migration from coastal regions [10]. Land use and diverse activities on the coast are pushed with the aid of high development to support network sports and boom the introduction of numerous spaces in coastal regions. This research focuses on the Subang coastal area because this area is vulnerable to rising sea levels due to global climate change, especially in the Sukasari and Blanakan sub-districts, which has an impact on coastal erosion [52]. Apart from that, intensive use of coastal areas changes the natural ecosystem of estuary and mangrove areas.

Over the past few decades, remote sensing technology and GIS applications have contributed significantly to geo-surveys, including coastline adjustment evaluation and

monitoring [11]. GIS and remote sensing technology enable satellite monitoring to examine an area without the need for direct fieldwork. GIS is an essential medium for detecting modifications in monitoring studies on a virtual temporal scale [12]. One of the uses of GIS in shoreline tracking is to evaluate temporal and spatial versions of the coastline [12]. Many researchers who use remote sensing have agreed on the performance of remote sensing in understanding numerous coastal processes and shoreline change dynamics [12]. In addition, remote sensing can also help develop coastal regions by looking at the coastal dynamics going on in a specific location.

Cloud computing is basically using internet-based services to support business processes. The word "Cloud" itself refers to the cloud symbol which in the world of information technology is used to describe the internet network (internet cloud). Cloud computing is a combination of the use of computer technology ('computing') and internet-based development ('cloud'). Cloud / cloud is a metaphor of the internet, as the cloud is often depicted on computer network diagrams, cloud (cloud) in cloud computing is also an abstraction of complex infrastructure that is hidden is a mode of computing where capabilities related to information technology are presented as a service (as a service), so that users can access them via the internet ("in the cloud") without knowledge of it, be expert with it, or have control of the technological infrastructure that assists it [53].

Landsat is a satellite released through NASA in 1972. Landsat offers remote sensing facts of the Earth's surface, making it easier for policymakers to determine guidelines based totally on environmental records and natural sources on the Earth's surface. Landsat benefits humans in various fields, specifically agriculture, climate, disasters, ecosystems, strength, fires, forestry, human fitness, populace growth, and water. Landsat satellite facts are open, admission to, and can be accessed by everybody via the official USGS or NASA portal.

Information about coastal dynamics and coastline modifications is essential for assessment and healing plans for coastal regions that are changing dynamically. The position of cloud computing-based geospatial generation for modified land analysis is one activity that indicates mitigation efforts across the coastal region of Subang Regency. Therefore, studies on coastal dynamics in the Subang Regency area are carried out to monitor those coastal dynamics. The research is predicted to be used as consideration for choice-makers and future research.

## **2 Methods**

### **2.1 Study area**

The research location is located on the coast of Subang Regency, West Java Province, with a total coastal area of 333.57 km<sup>2</sup> or around 16% of the entire Subang Regency [13] (Figure 1). Subang Regency borders directly on the North Java Sea, Indramayu Regency in the East, Sumedang Regency in the Southeast, West Bandung Regency in the South, and Purwakarta Regency and Karawang Regency in the West. Geographically, the Subang Regency area is located between 6°11'S - 6°49'S and 107°32'E - 107°55'E, with a district area of 2,051.76 km<sup>2</sup>. Apart from that, this research location is near a mangrove forest area used to protect critical genetic resources, one of which is used to develop pond cultivation businesses. This research take place in April - August 2023.

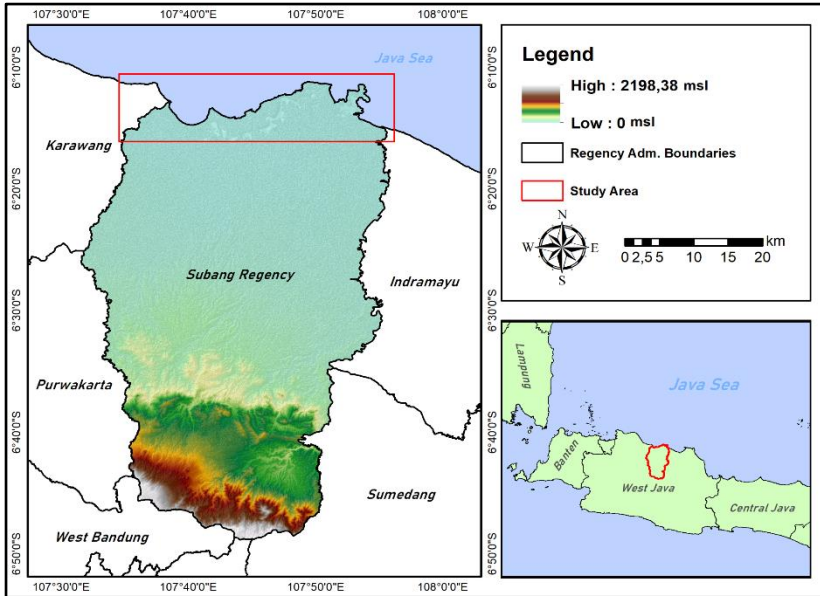


**Fig. 1.** Research location map.

## 2.2 Data and Data Analysis

The data used in this research is divided into several data, namely satellite data and classification data (training and validation) (Figure 2). This analysis also used training data that were retrieved and determined on the platform (Table 1). This research uses Landsat collection satellite data for satellite data, which can provide image data of the earth's surface from the 1980s until now with various generations of launches. This research was done considering that the monitoring target refers to every decade, starting from 1990, 2000, 2010, and 2020, until the latest condition coverage, 2023.

This research uses primary data originating from the Landsat satellite. Landsat is the oldest Earth surface monitoring satellite launched by National Aeronautics and Space Administration. Landsat can identify the earth's surface equipped with sensors that produce low-resolution images of 4 - 30 meters [14]. This research uses a collection of Landsat image data, including Landsat-5 (1990, 2000, 2010), Landsat-8 (2020), and Landsat-9 (2023). This image was analyzed via the Google Earth Engine (GEE) Platform. This platform is a cloud computing-based geospatial technology that offers many conveniences [15]. Previous study explains that this platform is integrated with various satellite imagery resources and is often used in various earth surface analyses [16]. According to [17], this geospatial platform uses Google storage resources to carry out geospatial analysis on a global scale.

This research data process uses an index algorithm to read differences in land cover on the earth's surface using wavelengths. [18] explains that various index algorithms, especially vegetation indices, were created to help identify vegetation on the earth's surface. The indexing algorithm used in this research uses 12 indices consisting of three indices: vegetation, water, and built-up land. There are seven vegetation type indices (Table 2), three water type indices (Table 3), and two built land type indices (Table 4). The involvement of

these various indices refers to the area's characteristics before and after coastal changes, for example, the presence of vegetation, wetlands, and the influence of soil.

Before detection, this research begins by determining the AOI (Area of Interest) and inputting it into the GEE platform. The detection process involving 12 indices is carried out by creating point areas on land and at sea. This change detection method has been carried out previously and refers to research [19] to determine areas affected by land changes due to fire. This research carries out a soil classification process with the help of training sample data, divided into two types of detection area, namely land (405) and ocean (300) (Table 1). In addition, this study involves other data sources such as Shuttle Radar Topography Mission data with a spatial resolution of 30 meters, as well as a combination of *Rupa Bumi Indonesia* map data [20], which can be seen through the following flow diagram.

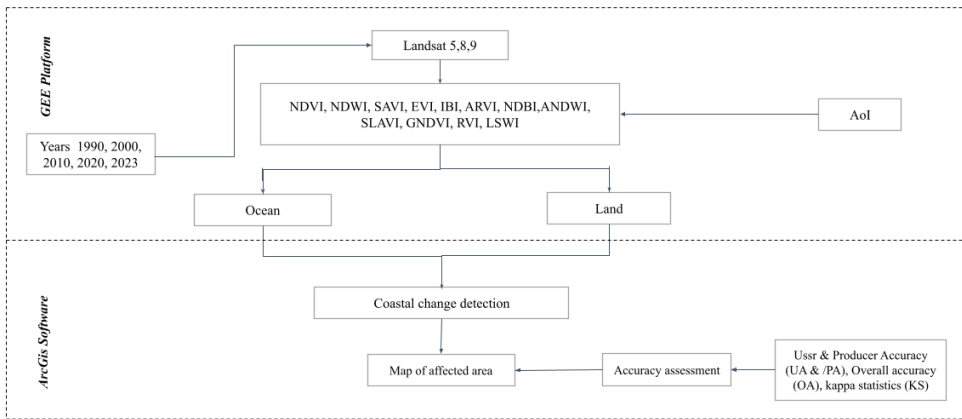


**Fig 2.** Research flowchart.

**Table 1.** Training sample data.

No	Years	Variable	
		Land	Ocean
1	1990	51	50
2	2000	80	87
3	2010	80	87
4	2020	97	38
5	2023	97	38
<b>Total training sample</b>		405	300

**Table 2.** List of vegetation indexes involved

No	Method	Formula	Reference
1	Normalized Difference Vegetation Index (NDVI)	$NDVI = \frac{NIR - Red}{NIR + Red}$	[22]

No	Method	Formula	Reference
2	Ratio Vegetation Index (RVI)	$RVI = NIR/Red$	[23]
3	Enhanced Vegetation Index (EVI)	$EVI = G ((NIR - Red) / (NIR + C1 \times Red - C2 \times Blue + L))$	[24]
4	Soil Adjusted Vegetation Index (SAVI)	$SAVI = 1.5 (NIR - Red) / (NIR + Red + 0.5)$	[25]
5	Atmospherically Resistant Vegetation Index (ARVI)	$ARVI = (NIR - (Red - (Blue - Red))) / (NIR + (Red - (Blue - Red)))$	[26]
6	Specific Leaf Area Vegetation Index (SLAVI)	$SLAVI = NIR / (Red + SWIR)$	[27]
7	Green Normalized Difference Vegetation Index (GNDVI)	$GNDVI = (NIR - Green) / (NIR + Green)$	[28]

**Table 3.** List of water indexes involved

No	Method	Formula	Reference
1	Augmented Normalized difference water index (ANDWI)	$ANDWI = (Blue + Green + Red - NIR - SWIR1 - SWIR2) / (Blue + Green + Red + NIR + SWIR1 + SWIR2)$	[29]
2	Normalized Difference Water Index (NDWI)	$NDWI = Green - NIR / Green + NIR$	[30]
3	Land Surface Water Index (LSWI)	$LSWI = (NIR - SWIR) / (NIR + SWIR)$	[31]

**Table 4.** List of built-up indexes involved

No	Method	Formula	Reference
1	Index-Based Built-up Index (IBI)	$IBI = ((NIR)/NIR + Red) + ((Green)/Green + SWIR1)$	[32]
2	Normalized Difference Built-up Index (NDBI)	$NDBI = (SWIR - NIR) / (SWIR + NIR)$	[33]

### 2.3 Google Earth Engine Platform: Classification coastal

Google Earth Engine (GEE) is an open-source cloud computing-based satellite image processing application acquired by Google in 2005. This application provides various types of satellite image data, such as LANDSAT, SENTINEL, NASA-NEX, and MODIS. Landsat images are selected and used automatically in the database provided by the GEE platform. The Landsat satellite image is subjected to time selection and cloud filters to obtain quality and cloud-free imagery. The selection is done successively in each classification year. The classification was carried out for three decades, namely 1990, 2000, 2010, 2020 and 2023. The classification was done by separating land and sea to obtain the actual coastline boundary. The classification process involves a classification algorithm and is assisted by an index algorithm (Table 2; Table 3; Table 4). The classification algorithm is the RF (random forest) algorithm, part of a machine learning (ML) based algorithm. Apart from that, the RF algorithm makes decisions on classification, referring to training data created previously for each classification year. Training data were retrieved and determined on the platform as many as 405 for land and 300 for sea (Table 1). A cross-section of the GEE platform used in all data analysis is presented in Figure 3.

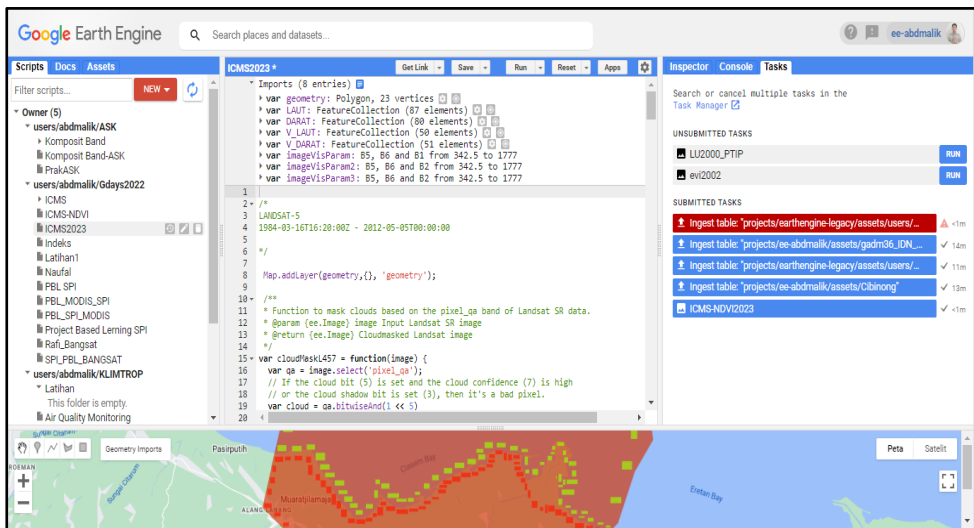


**Fig. 3.** Google Earth Engine (GEE) Platform

### 2.4 Accuracy assessment

Detection results using a remote sensing approach often produce spatial information that does not correspond to actual conditions. This detection requires systematic testing to test the level of accuracy of the results obtained through accuracy measurements [33][34]. In addition, this measurement is a treatment before the spatial information from this research is distributed to users [35]. This treatment is a determinant of the quality of the data produced. This research involves accuracy analysis, namely Overall Accuracy (OA; a), Kappa Statistics (KS; b), User Accuracy (UA; c), and Producer Accuracy (PA; d). This accuracy test involves validation data with total data amounting to 705 data taken through detailed imagery on the Google Earth Pro platform. This analysis is calculated by testing all coastal and coastline monitoring

results from the index used to obtain an index with a high accuracy level. The test results via the KS formula refer to the value interpretation class in Table 5 which has been created previously and is the most common in testing the level of data accuracy.

$$\text{Overall Accuracy (OA)} = \frac{1}{N} \sum_{i=1}^r X_{ii} \times 100\% \tag{1}$$

$$\text{Kappa Statistics} = \frac{N \sum_{i=1}^r X_{ii} - \sum_{i=1}^r X_{ii} (X_{i+} \times X_{+i})}{N^2 \sum_{i=1}^r X_{ii} (X_{i+} \times X_{+i})} \times 100\% \tag{2}$$

$$\text{User's Accuracy (UA)} = \frac{X_{ii}}{X_{+i}} \times 100\% \tag{3}$$

$$\text{Producer's Accuracy (PA)} = \frac{X_{ii}}{X_{i+}} \times 100\% \tag{4}$$

**Table 5.** Interpretation of kappa values.

Kappa value	Information
<0.00	Poor
0.00 – 0.20	Slight
0.21 – 0.40	Fair
0.41 – 0.60	Moderate
0.61 – 0.80	Substantial
0.81 – 1.00	Almost perfect

The validation data used in this research were obtained and determined from within the GEE platform by considering the characteristics of satellite images in the classification year. Observing image characteristics was done by setting the image composite on the RGB feature on GEE with various bands available on Landsat. Determining the location of the distribution of validation data is carried out by considering the distance and stretching from land to sea or perpendicular to the coastline. The distribution of validation points determined to test accuracy is presented in Figure 4.

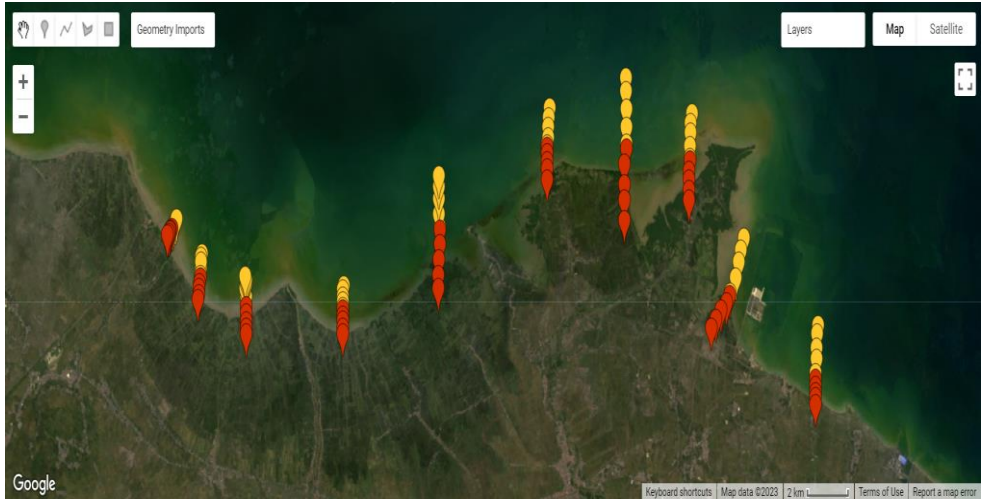


**Fig. 4.** Distribution of validation points (red = land validation, yellow = ocean validation)

### 3 Result and Discussion

#### 3.1 Classification result

##### 3.1.1 Coastal area classification capabilities

This research revealed the condition of the coastal area on the north coast of Subang Regency. This research succeeded because of the support of the cloud computing-based GEE platform, which produced maps of vulnerable land and ocean boundaries from 1990 to the present. This process is also based on the capability of the land classification algorithm, which involves the Random Forest (RF) machine learning classification algorithm. The classification process in the GEE platform has limited capabilities when viewed from the index algorithm that supports decision-making in the RF algorithm. In this research, the ability of each index algorithm is measured based on the VI (variable importance) method. This VI measurement feature is one of the advantages of the GEE platform for classifying satellite images. In this case, the VI value is shown in Figure 5.

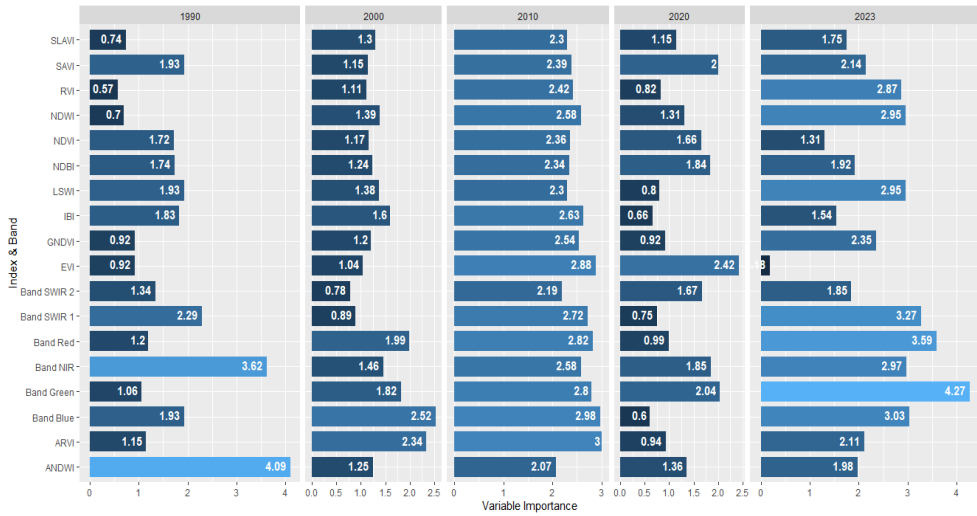


**Fig. 5.** Variable importance

The VI value in this study shows differences in the magnitude of the contribution of each index role in each classification year (Figure 5). Apart from that, the scale of the contribution to the VI calculation is different every year. For example, the value range scale in 1990, 2020 and 2023 is 0.574 - 4.092, 0.597 - 4.224, and 0.183 - 4.266, respectively. Meanwhile, in 2000 and 2010, the vulnerability was higher, namely around 78,334 - 252,443 and 2069.95 - 2999.72. If we look at the performance of each index, ANDWI is the index with the highest value in 1990, the blue band in 2000, ARVI in 2010, EVI in 2020, and the green band in 2023. Meanwhile, for the lowest contribution, the RVI index has a contribution value lowest in 1990, SWIR2 band in 2000, ANDWI in 2010, blue band in 2020, and EVI in 2023. The difference in the amount of contribution addressed by the VI value in each year is influenced by the characteristics of the pixel values in the training area in each classification. This difference is caused by the shape and location of the training area (polygon shape) being different in each classification year.

### 3.1.2 Accuracy classification of coastal areas

The results of the validation data obtained from Google Earth Engine were tested for the level of accuracy of the spatial information using a confusion matrix and shown in Figure 6. The analysis was conducted to ensure that spatial information regarding coastline changes that cause accretion and erosion in Subang Regency can be disseminated to the general public. The OA (overall accuracy), kappa coefficient, producer accuracy (PA), and user accuracy (UA) values, which are often seen as standards, are above 85% to be acceptable and are said to be at a comparable level of accuracy [37,38,39,40]. The analysis results interpret that the data on the dynamics of changes in the Subang Regency coastline has relatively high accuracy values, as shown in Figure 6. The highest accuracy values were obtained in 2023 and 2010 for each metric type (OA, kappa, PA, and UA), while the lowest value occurred in 2000. 2000 and 2008 were recorded as the worst years for horizontal accuracy, and Google made many improvements and developments to satellite imagery until 2018 [40]. The highest OA value is 1.00, and the lowest is 0.93. The highest kappa value was 0.99, and the lowest

was 0.85. The highest land and sea PA value was 1.00, and the lowest was 0.87. Meanwhile, the highest UA value is 1.00, and the lowest is 0.86 for land and sea. Based on this, the spatial information data on coastline changes from 1990 to 2023 for Subang Regency is worthy of acceptance and dissemination.

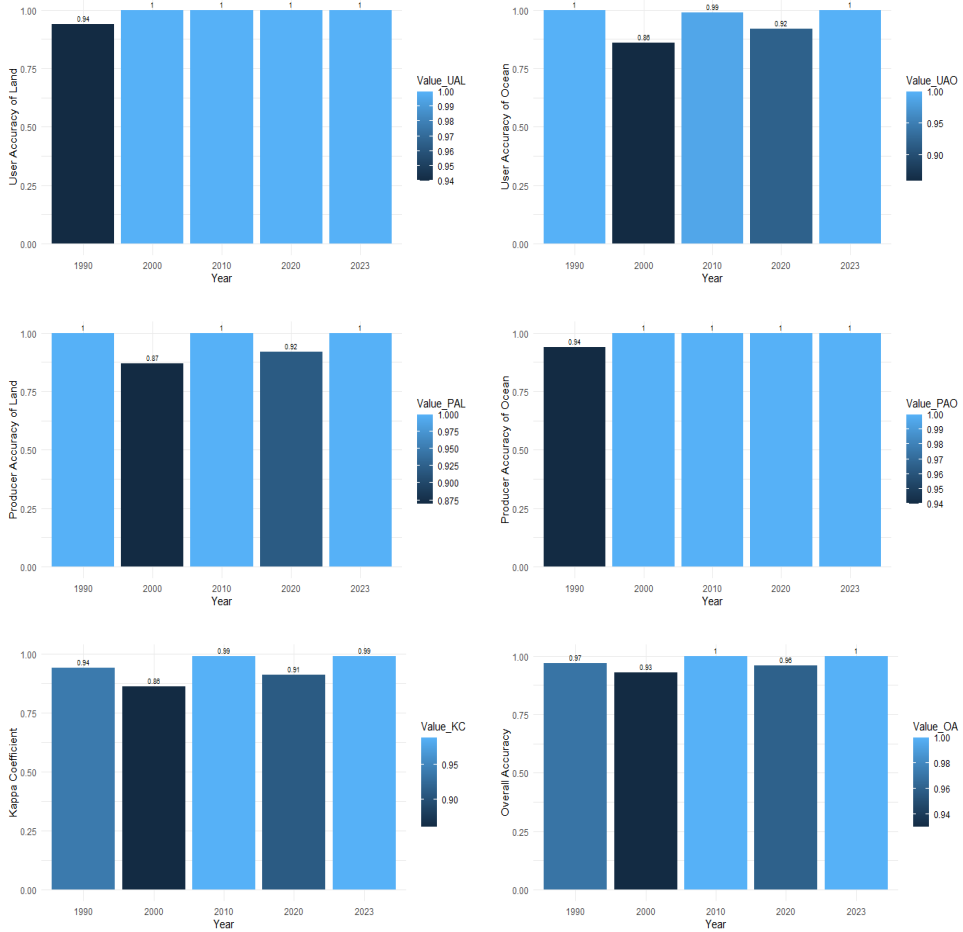


**Fig. 6.** The level of accuracy per year of classification

### 3.2. Coastal conditions, characteristics and structure

This study area's coastline shows a decline yearly (Figure 7). The decline or erosion on the Subang Coast occurred because it was related to the reduction in the area of mangrove forests, as happened in Sukasari District. There was an erosion process that dominated the entire coastal area of the district in the period 2001 to 2011 [41]. The decreasing density of mangrove forests has reduced their function as wave barriers, making erosion challenging to control. This degradation occurs due to human activities. The main factor causing mangrove logging to occur is economic pressure. The economic crisis that occurred several years ago has made people use mangroves as fuel or building materials. The uncontrolled conversion

of mangrove forest areas into other uses, such as fish and shrimp ponds, residential and industrial areas, and the overlapping use of mangrove forest areas for various development activities also causes the destruction of mangrove forests in the Subang area.

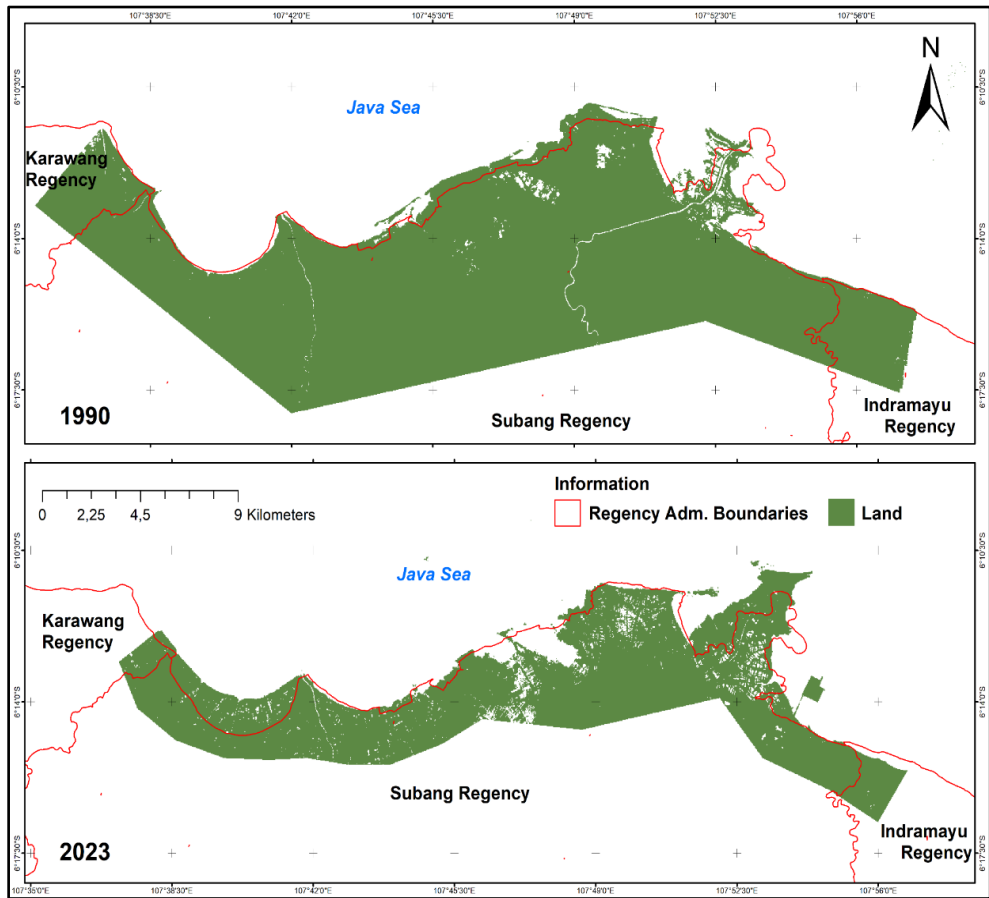


**Fig. 7.** Coastal classification at Subang Regency

Sandy beaches dominate the coastal area of Subang Regency. Apart from that, the coastal area of Subang Regency was also found to have muddy beaches with few mangroves, sea walls and rip-rap in some areas [41]. Pure mangrove areas that still survive are only found in estuaries or river deltas, such as Muara Ciasem, Blanakan, and also the Cipunegara delta, which is located around the villages of Blanakan, Langensari, Muara, and Patimban [41]. Based on direct monitoring results and information from local communities, most of the mangrove areas in the Subang area were deliberately cleared for unsustainable aquaculture (pond) purposes (Figure 8). This deliberate deforestation results in changes through erosion and accretion, which can increase vulnerability to natural disasters due to reducing mangroves as natural protection [42].



**Fig. 8.** Coastal Condition at Subang Regency

### 3.3. Coastline Change

The results of the analysis of changes in the coastline of Subang Regency during the period 1990-2023 were obtained from Landsat satellite image data. Data taken every decade is marked with a yellow line to depict the 1990 coastline, an orange line to depict the 2000 coastline, a green line to depict the 2010 coastline, a blue line to depict the 2020 coastline, and a purple line to depict the coast in 2023 (Figure 9). The results show that changes in the coastline occurred in the form of accretion in area I and area III, as well as erosion in area II. In 1990 the length of the coastline was 8.21 km, while in 2000 the length of the coastline changed to 6.52 km, resulting in a reduction in coastline of 16.89%. Furthermore, there was an addition to the coastline in 2010 to 8.14 km. Ten years later, in 2020, the length of the coastline changed to 8.81 km. However, in 2023 the length of the coastline will decrease to reach 6.89 km. However, in 2023 it is not yet known how much the coastline has changed, and in this study the calculation takes 10 years after the process of changing the coastline. That is because to get 4 years of change in an area requires 5 image data or 5 years, then for 5 years of change requires 6 years of data series. The highest coastline changes occurred in the 2020-2023 range as listed in Table 6, which indicates that there has been quite large accretion and erosion. The leading cause of coastline changes is the use of coastal areas to support community economic activities, resulting in erosion, accretion, sea water intrusion, reduction of mangrove forests and damage to coral reefs [43]. Land accretion that forms on the coast of Subang, especially in the Blanakan District, is caused by excess sediment runoff from the Ciasem River, which is then pushed by river flows towards the west [44]. Changes in coastal waters are also influenced by the dynamic interactions between water input from the sea and freshwater from rivers [45].

**Table 6** Coastline change in 1990 - 2023

Number	Year	Length (km)	Changes (%)
--------	------	-------------	-------------

1	1990	8.21	-16.89
2	2000	6.52	16.21
3	2010	8.14	6.66
4	2020	8.81	-19.16
5	2023	6.89	-

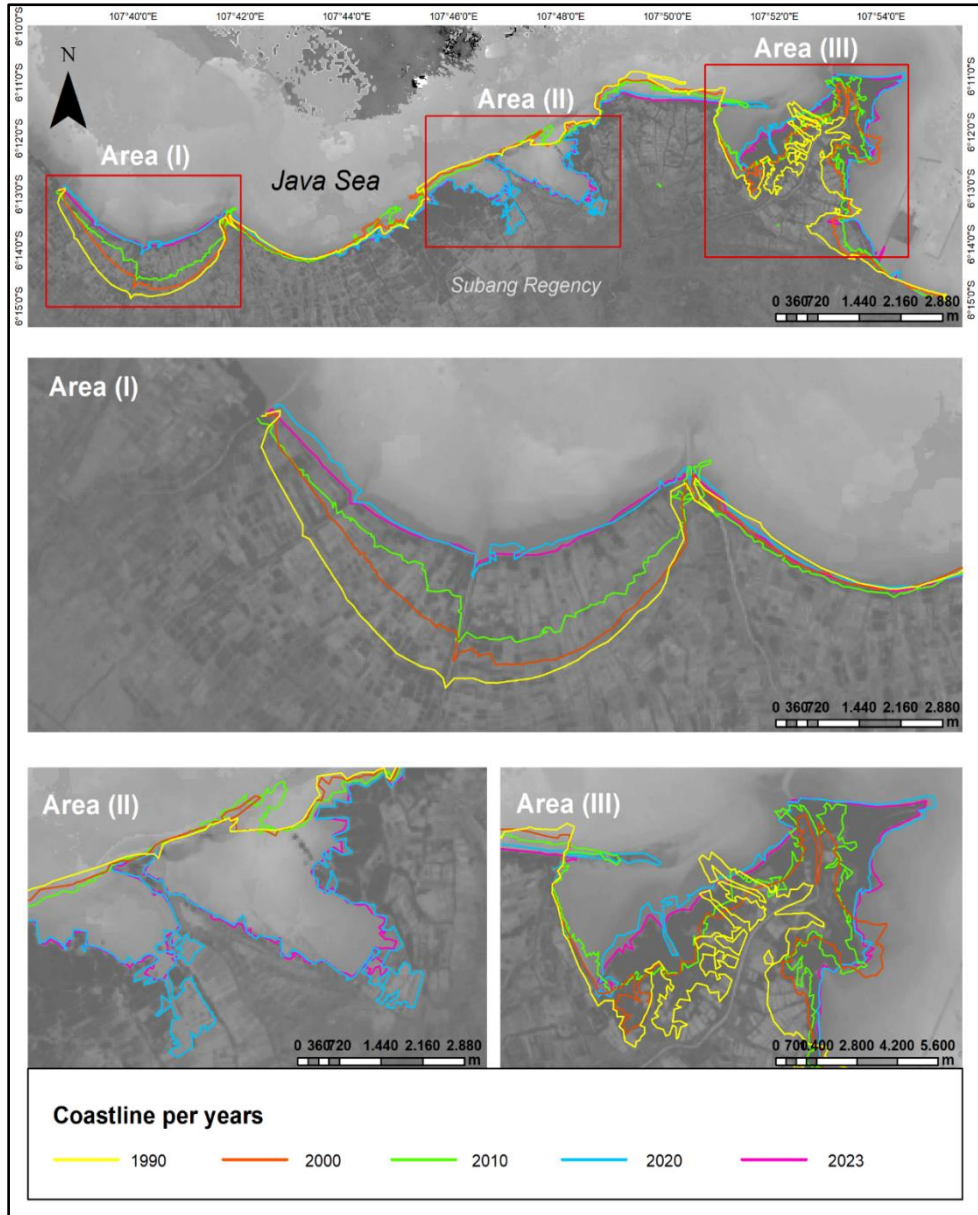


**Fig. 9.** Coastal change per years

### 3.4. Erosion and Accretion

Accretion is a natural process when sediment (sand, gravel, mud) accumulates in an area due to various processes, such as the deposition of alluvial material. Accretion can occur due to ocean currents, wind, or gravity. On the other hand, erosion is a natural process when material is lost from an area. Beach erosion involves material transport by waves, currents, or tidal action. Based on the results of the study conducted (Figure 10), the coastal areas of Subang Regency, which have experienced changes in land use, have experienced these two phenomena. From 1990 to 2023, there was abrasion of up to 980.4 ha and accretion of 1915.8 ha. The accretion process generally occurs in the eastern and western coastal areas, while erosion occurs in the central part of the coast. The accretion in the study area was caused by sediment runoff from the Ciasem River, which was then driven by longshore currents heading westward [54]. Previous research also states that sediment from the Cipunagara River has more impact than from the ocean did [55]. The accretion was also caused by the fact that the coast of Subang Regency to the west was sloping compared to the coast to the east, so the sediment originating from the Ciasem River was trapped in the bay of Blanakan District. Furthermore, it was reported that in 2018 many areas were used as fishponds in Blanakan District, thereby dominating the coastal accretion area. [43, 55]. It was also found that improvements in mangrove vegetation and the application of silvofishery by residents in the surrounding area supported accretion [55]. Improvements to coastal areas have also been carried out by planting mangroves by non-governmental organizations, companies, universities and other communities, but some of these were unsuccessful due to lack of monitoring.

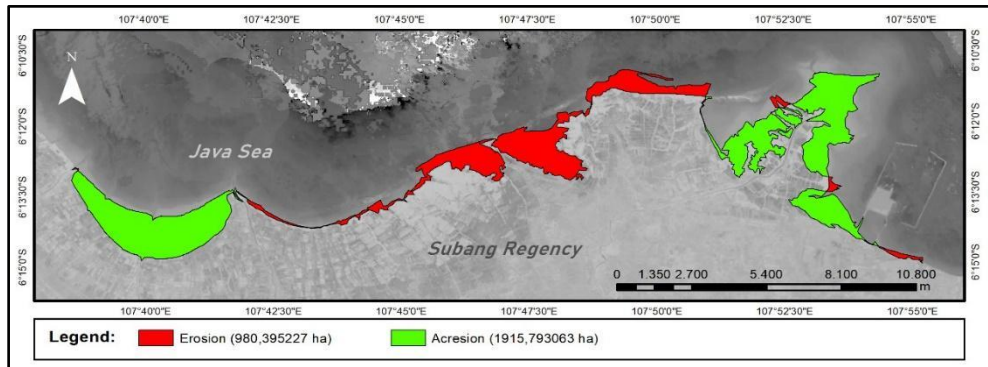


**Fig. 10.** Erosion and Accretion

Erosion occurred in several locations on the north coast of Subang Regency and was concentrated in the central area Legonkulon (Figure 10). Landsat satellite imagery has identified erosion from 1990 to now, amounting to 980.39 ha. This event was caused by the intensive opening of pond areas, which eroded the mangrove area (Figure 8). In 1990 our study area was almost covered by fishponds which were the main economic resource of the local people [59]. It is known that mangrove areas are a crucial and essential natural barrier in protecting land from fierce ocean waves. The cause of erosion in this area is due to the decline in land cover and density of the mangrove ecosystem area [53, 55]. The decline in mangrove areas is mainly due to unsustainable conversion of land into fish and shrimp ponds which began in the 1970s and became more massive in the 1990s. [57]. During the field inspection, areas were found that were indicated to be areas of erosion that reached far inland

and submerged the pond areas (Figure 11). The population is quite high on the coast of the Subang Regency study area, which indicates that many economic activities are concentrated in this area, such as crop production and fisheries. [43]. A report in 2010 stated that 37% of Subang's GDP came from the agricultural sector and decreased to 28% in 2017 [58, 59]. Erosion causes coastal disasters and impacts coastal communities continuously. Special attention is highly expected, for example, efforts to rehabilitate coastal areas to reduce the impact of marine disasters on coastal communities. Efforts to rehabilitate coastal areas can be carried out by revegetating mangrove forests that stretch along the coast [47,48,49,50]. As well as reducing access to land use in the form of fish ponds in the rehabilitation zone.



**Fig. 11.** Post-erosion coastal conditions

## 4 Conclusion

From 1990 to 2023, the coast in Subang Regency has undergone dynamic coastline changes. The west coast is an area that has accreted and a small part has experienced erosion, and the greatest erosion impact is in the middle of the coast. Accretion events in the western part, namely in the bay, could have occurred due to the influence of sediment runoff from a tributary of the Ciasem River, which empties into the bay. Cloud computing-based geospatial technology identifies the impact of change using Landsat-5, Landsat-8 and Landsat-9 imagery. Accretion in Blanakan Regency Bay averages 1915.8 ha. Most of the coast of Subang Regency experienced erosion on average 980.4. The results of the analysis interpret that the dynamic data of changes in the coastline of Subang Regency has a relatively high accuracy value, with the highest accuracy value obtained in 2023 and 2010 for each type of metric (OA, kappa, PA, and UA), while the lowest value occurred in 2000. Shifting The Farthest Coastline in Subang Regency, whether erosion or accretion, shows a very high correlation between the increase in years and the forward or backward movement of the coastline.

The author would like to thank the IPB SSRS Association for facilitating the authors starting from data collection (field survey), writing and publication.

## References

1. M. A. Marfai, B. Ahmada, B. Mutaqin, R. Windayati, *Geogr. Tech.* **15**, 106-116 (2020)
2. Supriyadi, N. Hidayati, A. Isdianto, *Prosiding Seminar Nasional Kelautan dan Perikanan III*; 2017; Madura, Indonesia. Madura : Program Studi Ilmu Kelautan Universitas Trunojoyo Madura (2017)
3. Darmiati, I. W. Nurjaya, A. S. Atmadipoera, *J. Ilmu Teknol. Kelaut. Tropis* **12**, 212 (2020)
4. I. D. A. Bernadetta, A. Laksono, D. T. N. Muhammad, I. F. Nurbaiti, N. N. Hanifah, O. S. Widiyanti, R. N. Junaedi, M. A. Marfai, *Maj. Geogr. Indones.* **35**, 75 (2021)
5. J. P. Mills, S. J. Buckley, H. L. Mitchell, P. J. Clarke, S. J. Edwards. *Earth Surf. Process. Landf.* **30**, 654 (2005)
6. G. A. Parvin, M. H. Ali, K. Fujita, M. A. Abedin, U. Habiba, R. Shaw, *Land Use Management in Disaster Risk Reduction: Practice and Cases from a Global Perspective*, (Springer, Tokyo, 2017)
7. Y. Asyiwati, H. Hindersah, *J. Phys. Conf. Ser.* **1469**, 012124 (2020)
8. O. Apena, D. M. Rondowunu, R. J. Poluan, *J. Spasial* **8**, 117 (2021)
9. S. B. Atmaja, D. Nugroho. *J. Kebijakan Perikan. Indones.* **3**, 101-113 (2017)
10. M. F. I. Rahman, H. Wibisana, S. Zainab. *J. Tek. Sipil* **16**, 144-156 (2020)
11. D. Apostolopoulos, K. A. Nikolakopoulos, *Eur. J. Remote Sens.* **54**, 240-265 (2021)
12. M. Yasir, H. Sheng, H. Fan, S. Nazir, A. J. Niang, M. Salauddin, S Khan, *IEEE Access* **8**, 180156-180170 (2020)
13. D. Sudinno, I Jubaedah, P. Anas, J. Penyuluh. *Perikan. Kelaut.* **9**, 17 (2015)
14. N. Suwargana, *J. Ilmiah Widya* **1**, 167-174 (2013)
15. O. Mutanga and L. Kumar, *Remote sens.* **11**, 591 (2019)
16. L. Kumar, O. Mutanga, *Remote sens.* **10**, 1509 (2018)
17. N. Gorelick, M. Hancher, M. Dixon, S. Ilyushchenko, D. Thau, R. Moore, *Remote Sens. Environ.* **202**, 8-27 (2017)
18. G. Rees, *The Remote Sensing Data Book* (Cambridge University Press, Cambridge, 2019)
19. S. T. Seydi, M. Akhoondzadeh, M. Amani, S. Mahdavi, *Remote Sens.* **13**, 220 (2021)
20. A. Ranti, R. Asy'Ari, T. H. Ameiliani, *IOP Conf. Ser.: Environ. Sci. Eur.* **959**, 012028 (2022)
21. J. W. Rouse jr, R. H. Haas, J. A. Schell, D. W. Deering, *NASA Technical Reports Server* **20**, 30-317 (1974)
22. C. F. Jordan, *Ecology* **50**, 663-66 (1969)
23. A. Huete, K. Didan, T. Miura, E. P. Rodriguez, X. Gao, L. G. Ferreira, *Remote Sens. Environ.* **83**, 195-213 (2002)
24. A. R. Huete, *Remote sensing of Environment* **25**, 295-309 (1988)
25. Y. J. Kaufman, D Tanre, *IEEE Trans. Geosci. Remote Sens.* **30**, 261-27 (1992)
26. L. Lyburner, P. J. Beggs, C. R. Jacobson, *Photogram* (2000)

27. A. A. Gitelson, Y. J. Kaufman, M. N. Merzlyak, *Remote Sens. Environ.* **58**, 289-98 (1996)
28. A. M. Rad, J. Kreidler, M. Sadegh, *Environ. Model Softw.* **140**, 105030 (2021)
29. B. C. Gao, *Remote Sens. Environ.* **58**, 257-66 (1996)
30. X. Xiao, S. Boles, J. Liu, D. Zhuang, M. Liu, *Remote Sens. Environ.* **82**, 335-48 (2002)
31. H. Xu, *J. Remote Sens.* **29**, 4269-76 (2008)
32. Y. Zha, J. Gao, S. Ni, *Int. J. Remote Sens.* **24**, 583-94 (2003)
33. G. M. Foody, *Photogramm. Eng. Remote Sens.* **70**, 627-633 (2004)
34. M. Diesing, S. L. Green, D. Stephens, R. M. Lark, H. A. Stewart, D. Dove, *Cont. Shelf Res.* **84**, 107-119 (2014)
35. R. G. Congalton, K. Green, *Assessing the Accuracy of Remotely Sensed Data: Principles and Practices, Second Edition* (CRC Press, Boca Raton Florida, 2009), 183
36. J. F. Brown, T. R. Loveland, D. O. Ohlen, Z. Zhu, *Photogramm. Eng. and Remote Sens.* **65**, 1069-1074 (1999)
37. P. Treitz, J. Rogan, *Prog. Plan.* **61**, 269-279 (2004)
38. McA Wilder, S. E. Franklin, J. C. White, J. Linke, S. Magnussen, *Int. J. Remote Sens.* **27**, 663-683 (2006)
39. J. J. Ge, J. G. Qi, B. M. Lofgren, N. Moore, N. Torbrick, J. M. Olson, *J. Geophys. Res.—Atmos.* **112**, D05107 (2007)
40. P. C. Nwilo, C. J. Okolie, J. C. Onyegbula, I. D. Arungwa, O. Q. Ayoade, O. E. Daramola, M. J. Orji, I. D. Maduako, I. I. Uyo, *Appl. Geomat.* **14**, 545-568 (2022)
41. A. N. Vina, A. Taofiqurohman, B. Koswara, *J. Perikanan dan Kelautan* **2**(3), 9-14 (2011)
42. D. N. Handiani, A. Heriati, W. A. Gunawan W, *Geomat. Nat. Hazards Risk*, (2022)
43. J. Kalther, A. Itaya, *J. Coast. Conserv* (2020)
44. Nandi, *Int. J. Conserv. Sci.* **5**, 387-396 (2014)
45. Nandi, G. Meriana, L. Somantri, *IOP Conf. Ser.: Earth Environ. Sci.* **47** 012017 (2016).
46. E. B. Barbier, *Frontiers in Ecology and the Environment* **4**, (2006)
47. R. Indarsih R, M. S. Masruri, *IOP Conf. Ser.: Earth Environ. Sci.* **271**, (2019)
48. P. Menéndez, I. J. Losada, Torres-Ortega, S. Narayan, M. W. Beck, *The Global Flood Protection Benefits of Mangroves* (Sci Rep 10, 2020)
49. D. A. Friess, B. S. Thompson, *Ecosystem-Based Disaster Risk Reduction and Adaptation in Practice* (Springer link, 2016)
50. R. Osti R, S. Tanaka, T. Tokioka, *Disasters*, (2009)
51. D. N. Handiani, S. Darmawan, R. Hernawati, M. F. Suryahadi, Y. D. Aditya, *REKA GEOMATIKA* (2), 61-71 (2017)
52. D. N. Handiani, S. Darmawan, A. Heriati, Y. D. Aditya, *J Kelautan Nasional* **14**(3), 145-154 (2019)
53. D. Aryani, I. T. Ningrum, *J. CCIT.* **5**, 145-167 (2011)
54. A. Taufiqurohman, M. F. A. Ismail, *J Trop Mar*, **4**, 82-87 (2012)
55. K. Munibah, A. Iswati, B. Tjahjono, *Globe* **12**, 151-159 (2010)
56. H. Kiswanto, Bogor Agricultural University [Academic thesis] (2015).
57. N. Sakuntala, Sylviani, *J. Soc. Study for Econ.* **11**, 281-293 (2014)
58. Subang Statistics Agency, *Subang in Figure 2010*, (Subang Statistics Agency, 2010)
59. Subang Statistics Agency, *Product Domestik Regional Bruto Kabupaten Subang Menurut Lapangan Usaha 2013-2017* (Subang Statistics Agency, 2017)
60. Subang Statistics Agency, *Subang in Figure 2018* (Subang Statistics Agency ,2018)